Predicting Dynamic Modulus of Asphalt Mixture Using Data Obtained from Indirect Tension Mode of Testing

Parnian Ghasemi[a,*], Shibin Lin[b], Derrick K. Rollins[c], R. C. Williams[a]

[a]*Department of Civil Engineering, Iowa State University, Ames, IA, USA*
[b]*Nondestructive Evaluation FHWA, Mclean, VA, USA*
[c]*Department of Chemical and Biological Engineering, Iowa State University, Ames, IA, USA*

Abstract

Understanding stress-strain behavior of asphalt pavement under repetitive traffic loading is of critical importance to predict pavement performance and service life. For viscoelastic materials, the stress-strain relationship can be represented by the dynamic modulus. The dynamic modulus test in indirect tension mode can be used to measure the modulus of each specific layer of asphalt pavements using representative samples.

Dynamic modulus is a function of material properties, loading, and environmental conditions. Developing predictive models for dynamic modulus is efficient and cost effective. This article focuses on developing an accurate Finite Element (FE) model using mixture elastic modulus and asphalt binder properties to predict dynamic modulus of asphalt mix in indirect tension mode. An Artificial Neural Network (ANN) is used to back-calculate the elastic modulus of asphalt mixtures. The developed FE model was verified against experimental results of field cores from nine different pavement sections from five districts in the State of Minnesota. It is demonstrated that the ANN modeling is a powerful tool to back-calculate the elastic modulus and FE model is capable of accurately predicting dynamic modulus.

Keywords: Dynamic modulus, Indirect tension mode of testing, Asphalt

---

[*]Parnian Ghasemi
  URL: `pghasemi@iastate.edu` (Parnian Ghasemi)

mixture, Finite element method, Artificial neural networks

1. Introduction

In order to predict pavement performance and service life, stress-strain behavior of asphalt pavement under repetitive traffic loading should be studied. One of the fundamental material properties of viscoelastic materials is the dynamic modulus which relates stress to strain [1, 2, 3, 4, 5]. Dynamic modulus is accepted by most pavement engineers as a critical parameter for flexible pavement design. As a stiffness indicator parameter, dynamic modulus is used in the Mechanistic-Empirical Pavement Design procedure [6, 7, 8].

The dynamic modulus test can be performed in two different test configurations, the uniaxial and indirect tension mode configurations. Both of these tests can be used in performance evaluation of the existing pavements. The uniaxial test configuration has the benefit of being simpler and less time consuming, while the indirect tension mode of testing is performed on a specific layer of a pavement section when the performance evaluation of a specific layer is of importance. Due to the multi-layer structure of the pavements, uniaxial text configuration is unable to evaluate each layer performance separately. Another issue with the uniaxial test configuration is the geometry requirement of the specimen. The test requires 6 inch tall specimens. Obtaining field cores with this dimension may not be possible in some cases with less than 6 inch thick Hot Mix Asphalt (HMA). Although indirect tension mode of testing can overcome this barrier, it is time consuming due to the manual tuning procedure and also the higher likelihood of damaging the specimens especially at higher temperatures.

Developing predictive models for dynamic modulus is always important and several predictive models are currently being used widely [9]. The basic concept of these models is predicting dynamic modulus value based on material components' properties including binder, aggregate, and mixture volumetric properties [9, 10, 11, 12, 13]. FE analysis is one way to develop such predictive models.

2

Finite element analysis has been used in modeling asphalt mixture with both elastic and viscoelatic assumptions [14, 15, 16, 17, 18]. Researchers have developed two-dimensional and three-dimensional FE programs to simulate asphalt mixture behavior [9, 19]. Finite element analysis is used to compare the material response with elastic and viscoelastic assumptions. Results indicate that the viscoelatsic assumption provides a more accurate estimation of pavement response [20, 21]. Although it has been shown that the finite element method is a powerful tool to simulate the viscoelastic behavior of asphalt mixtures [22, 23, 24], there has been a limited effort to use the application of FE modeling to simulate and further the understanding of the dynamic modulus test in the indirect tension mode.

In order to perform FE analysis, component properties of the pavement is required. Modeling viscoelastic behavior of asphalt mixtures requires defining both viscous and elastic properties of the material [22]. Elastic modulus can be used to describe the elastic behavior of the pavement as an input in FE analysis. In the absence of the test results this property can be back-calculated using pattern recognition techniques. Modern pattern recognition techniques can learn and recognize trends in data contributing to their current widespread use [25, 26]. These techniques learn the pattern from experimental data and design the computational models. One such approach, Artificial Neural Network (ANN), is an interconnected network of many simple processors [27, 28, 26, 29, 30]. Figure 1 presents the schematic architecture of a network with three layers. All networks consist of a set of processing units or neurons classified as input, hidden, and output neurons. Input neurons receive inputs from external sources and transfer it to the rest of the network. Hidden neurons receive input and transmit their computed output to the processing units within the network without any outside contact. Output neurons receive the input from the rest of the network and transform and send it to external receivers. The network can be trained by adjusting the network's weights and biases. Once the network learns the inputs/output(s) relationship, it can be used for further predictions [27].
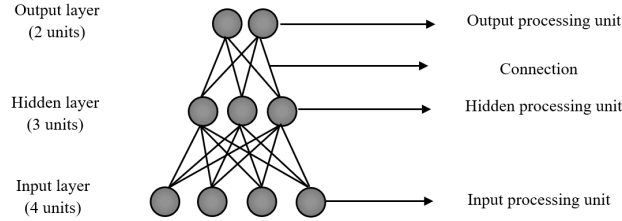
Figure 1: Schematic architecture of a network with three layers

This manuscript is organized as follows: the database creation procedure is presented in Section 2. Section 3 covers the model development. Results and discussion are presented in Section 4, followed by conclusions and recommendations in Section 5.

2. Database creation

Two separate databases are created for this research. The first one, database (a), is created using dynamic modulus values, complex shear modulus values, aggregate gradation, and mixture volumetric properties of twenty-seven field cores from nine different asphalt mixtures collected from five districts in the State of Minnesota. The summary information for each of these nine pavement sections is presented in Table 1.

The field samples for dynamic modulus testing are 6 inches (152.4-mm) in diameter and about 1.5 inches (38.1-mm) in thickness. The dynamic modulus test in indirect tension mode is performed at three temperatures (0.4, 17.1, and 33.8 $°C$) and nine loading frequencies (25, 20, 10, 5, 2, 1, 0.5, 0.2, 0.1 Hz)[1, 31]. Figure 2 illustrates the dynamic modulus test configuration in indirect tension mode of testing.

In order to obtain binder properties for each pavement group, binder extraction is done according to ASTM D7906(2014). The extracted binder then is recovered for testing following ASTM D2172(2011). A random number generator is used to select one sample from each pavement section for the binder
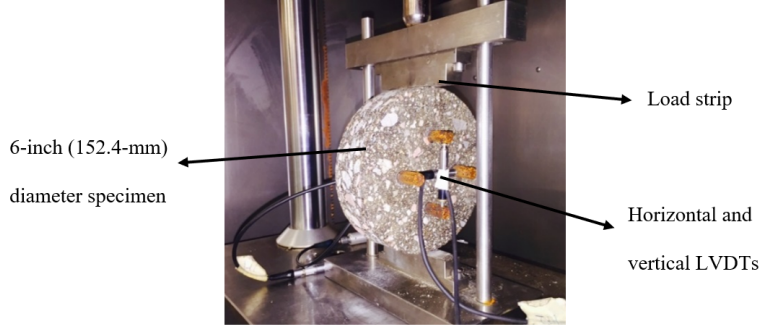
4

Figure 2: IDT dynamic modulus test setup

extraction and recovery. The binder dynamic shear test is performed at the same test temperatures and loading frequencies as the mixture dynamic modulus test. It should be mentioned that unlike the modified Witczak model, in the present research a consistent definition of frequency is used [32], that in order to predict the dynamic modulus value of an asphalt mix for example at 4 $°C$ and 25 Hz, one should input in the model the complex shear modulus of asphalt binder, $|G^*|$, at 4 $°C$ and 25 Hz. Using the laboratory test results on 27 specimens, a database of 243 data points is created for subsequent use in the FE analysis. The calculations are based on a linear viscoelastic solution for the IDT dynamic modulus test. All of the calculations are done based on the last five loading cycles. The applied sinusoidal loading can be expressed as shown in Eq. 1

$$P = P_0(cos\omega t + isin(\omega t)) \tag{1}$$

where P_0 is the amplitude of the sinusoidal load and ω is the loading frequency. Due to the load, a specimen will have a vertical and horizontal displacement which can be obtained from Eq. 2 and Eq. 3, respectively

$$V(t) = V_0 sin(\omega t - \phi) \tag{2}$$

$$U(t) = U_0 sin(\omega t - \phi) \tag{3}$$

where V_0 and U_0 are the constant amplitudes of vertical and horizontal displacement, respectively. The dynamic modulus can be obtained from Eq. 4

$$|E^*(\omega)| = \frac{2|P_0|(\beta_1\gamma_2 - \beta_2\gamma_1)}{(\pi a d)(\gamma_2|\bar{V}_0| - \beta_2|\bar{U}_0|)} \tag{4}$$

where β_1, β_2, γ_1 and γ_2 are geometric coefficients which depend on the specimen size and gage length and are obtained from Eq. 5 to Eq. 8 [33].

$$\beta_1 = -\int_{-l}^{l} n(y)dy - \int_{-l}^{l} m(y)dy \tag{5}$$

$$\beta_2 = \int_{-l}^{l} n(y)dy - \int_{-l}^{l} m(y)dy \tag{6}$$

$$\gamma_1 = \int_{-l}^{l} f(x)dx - \int_{-l}^{l} g(x)dx \tag{7}$$

$$\gamma_2 = \int_{-l}^{l} f(x)dx + \int_{-l}^{l} g(x)dx \tag{8}$$

where,

$$n(y) = tan^{-1}\left(\frac{1 + \frac{y^2}{R^2}}{1 - \frac{y^2}{R^2}}tan\alpha\right) \tag{9}$$

$$m(y) = \frac{(1 - \frac{y^2}{R^2})sin2\alpha}{1 - 2(\frac{y^2}{R^2})cos2\alpha + \frac{y^4}{R^4}} \tag{10}$$

$$f(x) = \frac{(1 - \frac{x^2}{R^2})sin2\alpha}{1 - 2(\frac{x^2}{R^2})cos2\alpha + \frac{x^4}{R^4}} \tag{11}$$

$$g(x) = tan^{-1}\left(\frac{1 - \frac{x^2}{R^2}}{1 + \frac{x^2}{R^2}}tan\alpha\right) \tag{12}$$

where y and x are the vertical and horizontal distances from the specimen center respectively, R is the specimen radius, α is the radial angle, and l is half of the gage length.

The second database, database (b), is created using field cores taken from 20 different pavement sections in the States of Iowa, Wisconsin, and Minnesota.

Table 1: Pavement sections information (* M/O = Mill and Overlay; ** O/L = Overlay)

Group No.	Section	MnDOT District	Construction Year	Construction Type
1	TH 220	2	2012	3" M/O*
2	CSAH 10	1	2012	1.5" O/L** on old AC
3	TH27	3	2010	3" M/O
4	TH 9	2	2011	3" O/L on reclaimed AC
5	TH 28	4	2012	4.5" M/O
6	TH 6	2	2010	1.5" M/O
7	TH 10	4	2013	3.5" M/O
8	CSAH 30	Metro	2012	6" M/O
9	TH 10	3	2005	4" M/O (sealed cracks)
10	TH 10	3	2005	4" M/O (cracks not sealed)

This database is used to back-calculate the elastic modulus based on the material components' properties. Dynamic modulus testing was performed on these specimens at four different temperatures and five loading frequencies. The interconversion method between linear viscoelastic material properties [34] is used and presented in Eq. 13

$$E' = |E^*|cos(\phi) \tag{13}$$

where E' is the storage modulus, $|E^*|$ is the dynamic modulus, and ϕ is the phase angle. The storage modulus is an indicator of elastic behavior of the material and is used as an estimation of the elastic modulus. Aggregate gradation, asphalt binder shear properties, and volumetric properties of the mixture are retrieved from historical documents and a total of 240 data points for elastic modulus, aggregate, asphalt binder, and mixture properties are developed.

3. Model Development

3.1. Back-calculation of the asphalt mixture elastic modulus in database (b)

An ANN is an interconnected collection of processing elements [35] and can be trained to approximate a complex, nonlinear function through repeated exposure to produce meaningful solutions to the problem [28, 36, 37, 38]. The multi-layer structure of the network ensures non-linear mapping of inputs to outputs.

7

A useful application of neural networks is in back-calculation procedures where it can be trained to approximate the inverse function by repeatedly showing it forward problem solutions. Once a network has learned the pattern of inputs/output(s) relationship, it can predict new conditions [27].

Using database (b), a three-layer feed-forward error-back propagation network is trained. The network is composed of an input layer, an output layer and one hidden layer and developed using the MATLAB program [39]. Figure 3 presents the schematic architecture of the network having eight neurons (nodes) in the input layer, 10 neurons in the hidden layer and one neuron in the output layer. Selection of the number of hidden neurons is based on a trial-and-error optimization procedure balancing between the cost function and computational time. Selection of the input variables is based on the existing literature. There are several predictive models for dyanmic modulus that can predict the modulus value using material components' properties [6, 11, 10, 32]. Researchers developed a network which is able to predict the value of dynamic modulus more accurate than modified Witczak model [32]. Their predictive models use the same input variables as modified Witczak model. The input variables are including aggregate gradation, binder shear properties, binder content, and air void. In the present study, same input variables are used with an additional step of converting dynamic modulus to the elastic modulus.

Database (b) is randomly divided into three categories. Seventy percent of the data points is presented to the network during the training procedure. The Levenberg-Marquardt method is used as the training algorithm [40]. Fifteen percent of the data points is used for the validation of the fitting, and the rest of the data is used for testing. The training procedure starts with adjusting the initial values of the network's weights and biases to obtain a reasonable output and continue to modify the network by minimizing the mean squared residuals (MSE). The input of each processing element (x_i) is multiplied by an adjustable connection weight (w_{ij}). At each processing element, the weighted input signals are summed and a threshold value (B_0) is added. This combined input is then passed through a non-linear transfer function ($f(.)$) to produce the output of
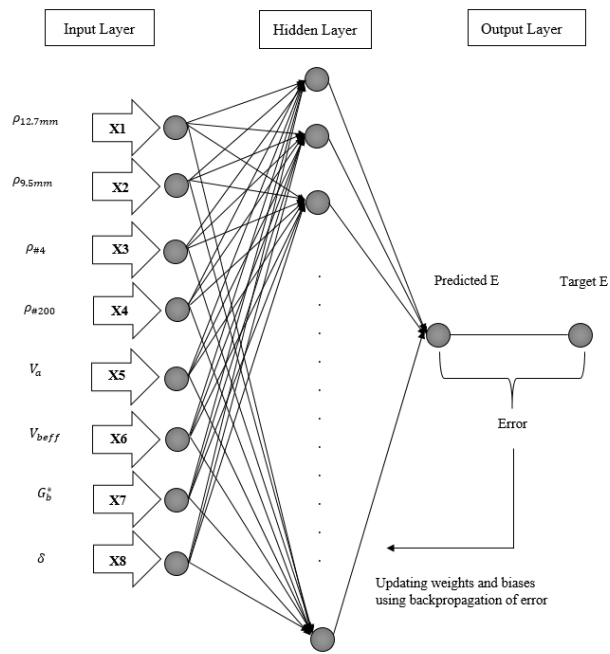
8

Figure 3: Schematic architecture of a network with three layers

the first layer (ν_j), forming the input to the next layer. The network adjusts its weights on the presentation of a training dataset and uses a learning rule to find a set of weights that will produce the input/output mapping that results in the smallest possible error. This process is called "learning" or "training". In order to prevent overfitting, supervised learning procedure is used by means of having a validation subset. Once the training phase of the model has been successfully accomplished, the performance of the trained model must be validated using an independent validation set. After applying modifications and adjustments to the network's weights and biases the performance of the network will be examined by an independent testing set [27, 41, 42].

The output ν_j from the jth hidden nodes is given by

$$\nu_j = f(x_i, W_{ij}), \quad i = 1, ..., 8 \quad and \quad j = 1, ..., 10 \tag{14}$$

and the single output $\hat{y}$ is:

$$\hat{y} = f_2\left(f_1(\nu, W_j)\right). \tag{15}$$

Then the expression of $\hat{y}$ as a function of x becomes a complicated nonlinear regression function with the j sets of weights, as parameters. and for each j,

$$\nu_j = f_1(B_{H_j} + W_{ij}x_i). \tag{16}$$

So a general form of the feed forward neural network is described in Eq. 17:

$$\hat{y} = f_2\left\{B_0 + \sum_{j=1}^{n}\left[W_j \cdot f_1\left(B_{H_j} + \sum_{i=1}^{m} W_{ij}x_i\right)\right]\right\} \tag{17}$$

where B_0 is bias at output layer (just one neuron at this layer), W_j is weight of connection between neuron j of the hidden layer and output layer neuron, B_{H_j} is bias at neuron j of the hidden layer (for $j = 1$ to 10), W_{ij} is weight of connection between input variable i (for $i = 1$ to 8) and neuron j of the hidden layer, x_i is input parameter i, $f_1(t)$ is transfer function of the hidden layer, and $f_2(t)$ is transfer function of the output layer.

Both transfer functions $f_1(t)$ and $f_2(t)$ used in this research are sigmoid functions as defined by Eq 18:

$$f_k(t) = \frac{1}{1 + e^{-t}} \quad for \quad k = 1, 2. \tag{18}$$

For the training set, the training procedure starts with adjusting the initial values of the network's weights and biases to obtain a reasonable output and continue to modify the network by minimizing the value of the MSE. The iteration continues until the convergence criterion is met as previously described. Once the network is trained and learns the pattern, it will be used to predict the elastic modulus values using database (a). The predicted elastic modulus will be used as an input in the finite element analysis.

3.2. Finite element analysis

Finite element analysis is performed using a multi-purpose FE software, ABAQUS [43]. ABAQUS has a module for viscoelastic materials which can be used for modeling asphalt mixture. A disk-shape geometry with the same dimensions as the laboratory HMA samples is created. The specimen is restricted at the bottom from movement and rotation in all directions and a sinusoidal uniform pressure is applied on top of the specimen via a loading strip. In order to determine the load magnitude, different load amplitudes are studied and adjusted so that the observed horizontal and vertical strains in the center area of the specimen remain between 60 and 80 micro-strain and below 100 micro-strain, respectively [1]. The mesh element type used for this model was from a 3D stress family, an eight-node linear brick, with reduced integration and hourglass control (C3D8R). Figure 4 shows the model geometry, boundary conditions, and mesh.

There are several methods to define material properties in ABAQUS. Asphalt binder complex shear modulus test results are used in this paper. ABAQUS has a built-in function which transforms the shear modulus into a Prony series. The Prony series is an exponential expansion often used to describe the relaxation
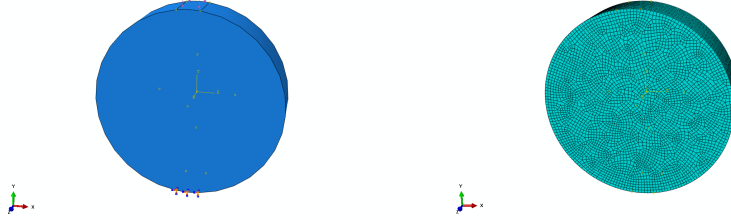
Figure 4: Geometry, load, and boundary conditions (on the left), and mesh (on the right) used in FE analysis.

modulus of a viscoelastic material [44]. The data is normalized as the ratio of the modulus at individual times to the long-term modulus.

The material temperature dependency should be defined in the model. Temperature dependency is defined using the shift factors obtained from Williams-Landel-Ferry (WLF) equation [14, 44, 45] which is presented by Eq. 19.

$$log(\alpha_T) = \frac{C_1(T - T_s)}{C_2 + T - T_s} \tag{19}$$

where α_T is the WLF shift factor, T is the temperature of each individual test, C_1 and C_2 are the constants and T_s is the reference temperature which is 17.1 $°C$ in this research (Shear modulus values at 0.4 $°C$ and 33.8 $°C$ are shifted according to the reference temperature). For each individual temperature after determining C_1 and C_2 and shifting all of the complex modulus data according to the reference temperature, the value of these two constants at the reference temperature are used in the model as inputs. Poisson's ratio is assumed to be 0.25. The selection of this value is based on material behavior at 17.1 $°C$. A sensitivity analysis on the Poisson's ratio impact on the dynamic modulus value was conducted and the results demonstrated a very negligible effect exists. As described earlier in the previous section, the elastic modulus of the material is predicted using the trained neural network. The predicted elastic modulus is used in the model as an input.
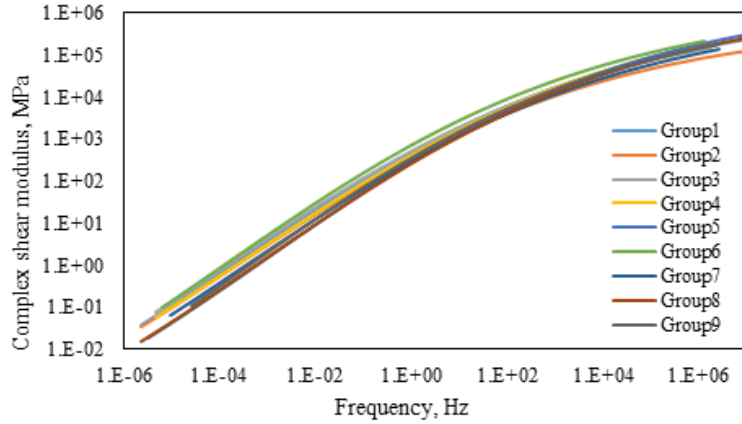
12

Figure 5: Complex shear modulus master curves obtained from extracted and recovered asphalt binders of nine pavement sections

4. Results and discussion

Results of the laboratory tests, elastic modulus back-calculation, and finite element analysis are presented in this section. The capability and accuracy of the developed model in predicting dynamic modulus values is also evaluated.

4.1. Laboratory testing

The results of complex shear modulus test, dynamic modulus test, aggregate gradation, and mixture volumetric measurements are presented in this section. Complex shear modulus values are determined and are used to create master curves. The master curves for the nine groups are presented in Fig. 5.

To calculate dynamic modulus test results geometric coefficients, β_1, β_2, γ_1, γ_2, are calculated for specimen diameter of 152.4 mm (6") and gage length of 65 mm (2.56") and presented in Table 2. The average dynamic modulus values for three specimens per group for the nine pavement groups are presented in Table 3.

As described earlier, the results of dynamic modulus testing, complex shear modulus testing, aggregate gradation, and volumetric properties are used to develop database (a). Mixture volumetric properties are presented in Table 4.

13

Table 2: Geometric coefficients

Specimen Diameter (mm)	Gauge Length (mm)	β_1	β_2	γ_1	γ_2
152.4	65	0.0262	-0.0078	0.0063	0.0206

Table 3: Average dynamic modulus values for nine pavement groups of database (a)

Group No.	Temp.	25 Hz	20 Hz	10 Hz	5 Hz	2 Hz	1 Hz	0.5 Hz	0.2 Hz	0.1 Hz
1	0.4	20425	20252	22008	18619	17501	16210	14836	13512	11995
1	17.1	12573	12510	11315	9360	7537	6399	5081	3928	3104
1	33.8	4798	4718	3462	2495	1680	1193	1000	656	502
2	0.4	14822	17293	18841	17532	15858	14445	13132	11527	10191
2	17.1	9768	9528	8905	7362	5751	4768	3934	2958	2386
2	33.8	3157	2629	2077	1691	1203	982	779	631	593
3	0.4	20128	19719	19727	18427	16927	15917	14710	13495	12285
3	17.1	15137	15679	14442	12439	10730	9330	7999	6584	5652
3	33.8	5769	5424	4419	3379	2353	1813	1394	1010	832
4	0.4	21585	20264	19523	18049	16166	14767	13283	11639	10277
4	17.1	13191	12485	11481	10044	7754	6457	5244	4008	3281
4	33.8	5083	4877	3591	2718	1897	1443	1145	820	664
5	0.4	22738	16279	16353	14882	13157	11970	10627	9074	7931
5	17.1	9634	8889	7820	6369	4802	3875	3032	2244	1638
5	33.8	3172	2882	2180	1621	1183	1005	950	750	607
6	0.4	22324	23397	21829	20659	18753	17531	16515	14680	13266
6	17.1	14264	13526	13312	11314	8720	7472	6167	4887	3921
6	33.8	5512	5241	4146	3028	1995	1520	1138	766	557
7	0.4	26413	22774	22624	21734	20130	18938	17544	15723	14373
7	17.1	13950	13122	12836	10514	8153	6782	5470	4310	3459
7	33.8	4486	4161	3377	2440	1658	1256	976	710	519
8	0.4	24299	22946	22938	21377	20027	18331	16929	15092	13813
8	17.1	12588	12151	10727	8796	7034	5822	4758	3653	2935
8	33.8	4627	4006	3347	2695	1906	4886	1320	1171	1061
9	0.4	20954	19559	20433	18470	16892	15498	14046	12499	11149
9	17.1	11719	11584	10429	8377	6339	5194	4020	2965	2147
9	33.8	4832	4195	3067	2171	1539	1198	919	614	468

Table 4: Mixture volumetric propeeties for nine pavement groups of database (a)

Group No.	1	2	3	4	5	6	7	8	9
% RAP	23.8	23.3	37.2	26.2	23.8	36.4	23.3	11.4	45.3
% AC	4.5	5.2	5.6	4.8	4.8	4.9	5.6	5.3	5.0
% Vbeff	4.2	4.1	4.1	3.9	3.5	4.3	4.2	4.0	4.6
%VMA	13.5	13.5	13.6	13.1	12.5	13.9	13.7	13.4	14.4
% VFA	70.3	70.4	70.6	69.6	68.1	71.2	70.8	70.2	72.3
Gmb	2.315	2.315	2.315	2.315	2.315	2.315	2.315	2.315	2.315
Gmm	2.406	2.458	2.510	2.479	2.635	2.458	2.479	2.510	2.437
% VA	4.010	3.996	3.998	3.982	3.988	4.003	4.000	3.993	3.989

Table 5: Network's input variables information

Variable	Values in the database			
	Maximum	Minimum	Average	Std. Dev
Complex Modulus (Mpa)	1065.6	0	45.4	117.2
Phase angle (degree)	79.2	28.2	52.9	11.5
Vbeff%	5.6	4.5	5.1	0.4
Va%	4.0	4.0	4.0	0
% Passing 1/2"	96.4	87.2	93.9	2.6
% Passing 3/8"	87.3	73.7	81	4.1
% Passing #4	63.8	48.2	54.1	5.3
% Passing #200	6.2	3.1	3.8	0.9

4.2. Back-calculation of the asphalt mixture elastic modulus in database (b)

The database (b) is created using elastic modulus (converted from dynamic modulus), asphalt binder properties, aggregate gradation, and mixture volumetric properties. The database is used to develop a neural network. A summary of the input variables used in the network and a descriptive measurement of them is presented in Table 5.

As mentioned previously, the successfully trained three-layer ANN can be presented as in Eq. 17. For ease of use and wider reproduction, the connection weights and biases are presented using the following matrices:

$$
W_{\mathrm{ij}} =
\begin{bmatrix}
2.029 & 0.694 & -0.925 & 1.324 & 0.813 & 2.011 & -2.524 & -3.292 \\
-1.204 & 1.141 & 1.162 & 2.611 & 3.966 & 1.076 & -3.257 & 3.474 \\
2.135 & -1.270 & -0.277 & 0.179 & 0.683 & -1.184 & 1.174 & -3.481 \\
-0.549 & -4.837 & -2.383 & 0.794 & -2.491 & -1.766 & 1.930 & 5.408 \\
-0.777 & 1.006 & 2.255 & 0.436 & -1.330 & 1.137 & -2.658 & 4.933 \\
-0.757 & 1.685 & -1.889 & 1.674 & -3.114 & -2.335 & -6.051 & 3.408 \\
1.902 & -4.753 & 2.162 & -1.423 & 3.355 & 3.591 & -3.999 & -4.170 \\
-0.908 & 1.131 & 1.281 & 2.445 & 1.158 & 0.550 & 4.798 & -1.167 \\
2.171 & 0.007 & -0.669 & -1.475 & 1.944 & -0.571 & -4.329 & -2.316 \\
-0.684 & 1.626 & 0.741 & 0.582 & 0.041 & -1.464 & 1.508 & -0.188
\end{bmatrix}
$$

$$
W_{j}^{T} =
\begin{bmatrix}
0.518 \\
-0.076 \\
0.614 \\
0.236 \\
0.082 \\
-0.244 \\
-0.280 \\
-1.012 \\
0.821 \\
2.000
\end{bmatrix}
, \quad
B_{\mathrm{Hj}} =
\begin{bmatrix}
-4.851 \\
5.433 \\
-0.647 \\
3.163 \\
-1.864 \\
-6.336 \\
4.520 \\
-5.244 \\
4.0312 \\
-2.220
\end{bmatrix}
, \quad
B_0 = [0.603]
$$

Accuracy of the network is evaluated and the results are presented in this section. The performance evaluation is based on the r_{fit} which is defined in Eq. 20

$$
r_{fit} = \frac{n \sum_{i=1}^{n} E_i \hat{E}_i - (\sum_{i=1}^{n} E_i)(\sum_{i=1}^{n} \hat{E}_i)}{\sqrt{n \sum_{i=1}^{n} E_i^2 - (\sum_{i=1}^{n} E_i)^2}\sqrt{n \sum_{i=1}^{n} \hat{E}_i^2 - (\sum_{i=1}^{n} \hat{E}_i)^2}} \tag{20}
$$

where r_{fit} is the correlation coefficient, E is the elastic modulus, and $\hat{E}$ is the predicted elastic modulus. Figure 6 presents the performance of the network for training, validation and testing subsets in terms of r_{fit}. The r_{fit} of 0.99 for testing, validation and testing subsets indicates that the ANN is capable
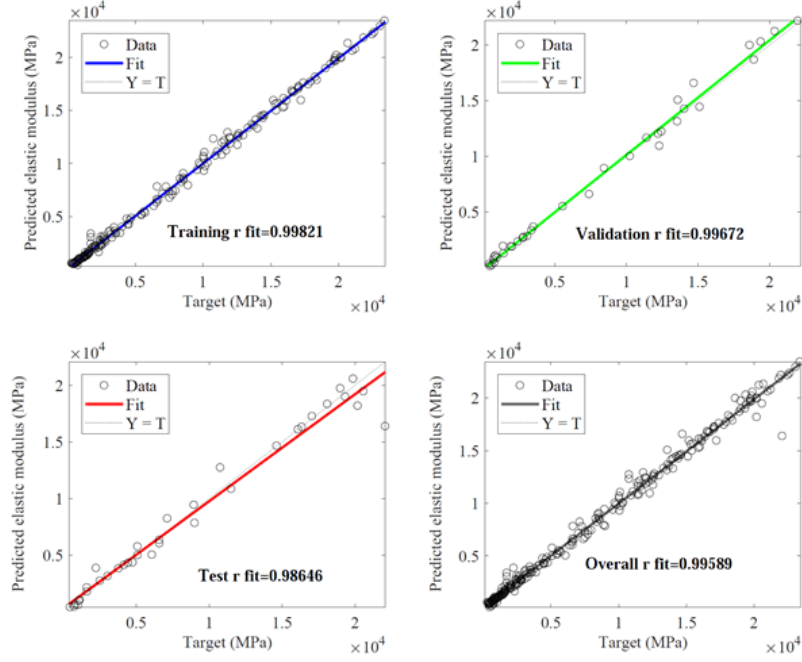
16

Figure 6: Performance evaluation of the network. The top-left graph indicates performance of the network in fitting to the training subset with r_{fit} of 0.99. The top-right graph indicates performance of the network for validation subset with $r_{fit}= 0.99$. The bottom-left graph indicates the performance of the network for testing subset with r_{fit} of 0.98. The bottom-right graph indicates the overall performance of the network.

of predicting the elastic modulus value of asphalt mixtures. The fact that the values of r_{fit} for all of the subsets are close assures that the over-fitting is not likely to happen in the supervised training procedure.

4.3. Finite element analysis

Results of finite element analysis is presented in this section. The deformed shape of the HMA specimen due to sinusoidal loading with the loading frequency of 25 Hz is presented in Fig. 7.

Vertical and horizontal stresses, S_{22} and S_{11}, and deformations, U_2 and U_1, of the specimen under the applied load are obtained for different loading frequencies. Complex modulus values for the nine different pavement groups
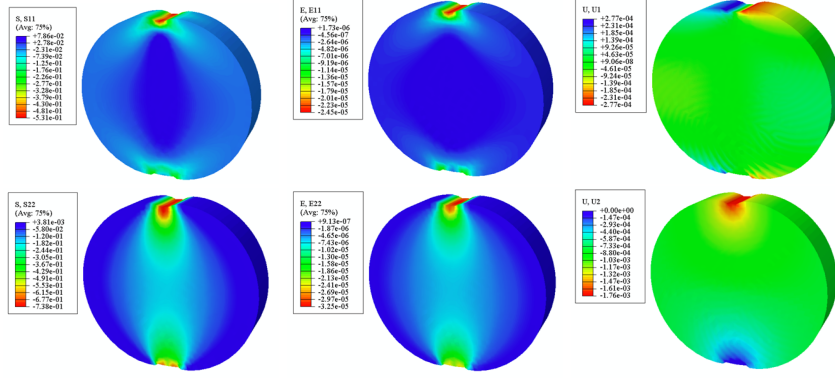
17

Figure 7: Finite element analysis results. From left to right, the top ones indicate stress, strain and deformation in horizontal direction and the from left to right, bottom ones indicate stress, strain and deformation in vertical direction respectively.

are calculated for each frequency using Eq. 21.

$$E^* = \frac{S_{11} - \nu S_{22}}{E_{11}} \tag{21}$$

where S_{11} is the horizontal stress along the x-axis, S_{22} is the vertical stress along the x-axis and E_{11} is the horizontal strain along the x-axis. The obtained modulus from Eq. 21 is the complex modulus of the material along the x-axis which is assumed to be not very different from the modulus along the y-axis. The dynamic modulus value is the amplitude of the complex modulus wave is presented in Eq. 23

$$E^* = |E^*|e^{(i\phi)} \tag{22}$$

where i is the imaginary number and ϕ is the phase angle. The predicted values of dynamic modulus were calculated and compared with laboratory test results. Figure 8 indicates a comparison between master curves obtained from experimental results and the ones obtained from the FE analysis. For all of the nine groups, the FE analysis was able to predict the dynamic modulus value.

Element size is an important factor in determining the accuracy of solution in the FE method. To converge the solution to the correct value, the mesh
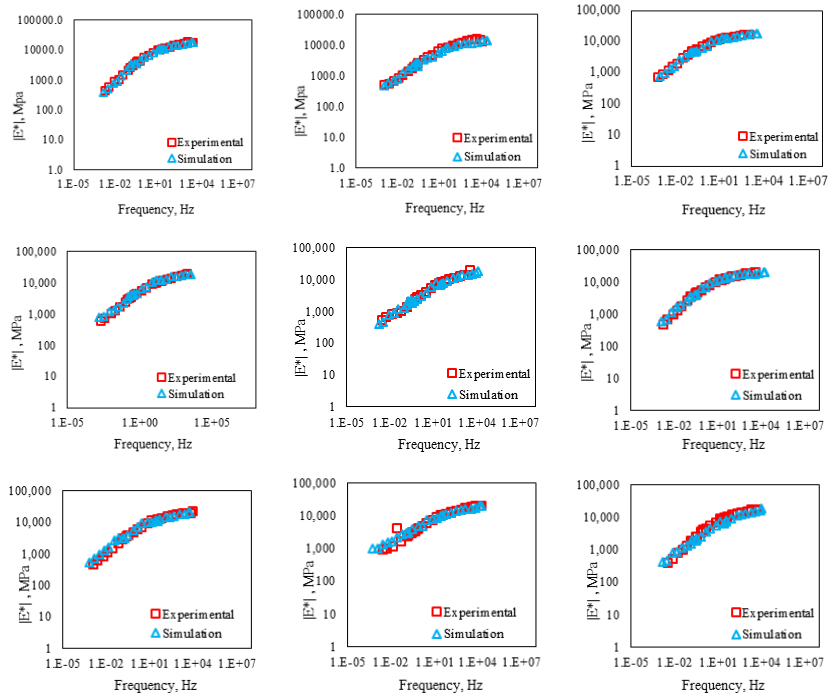
18

Figure 8: Comparison of master curves created using experimental results and simulation results for 9 different pavement sections. Master curves are ordered from left to right so the very top-left one belongs to Group 1 and the very bottom one belongs to Group 9
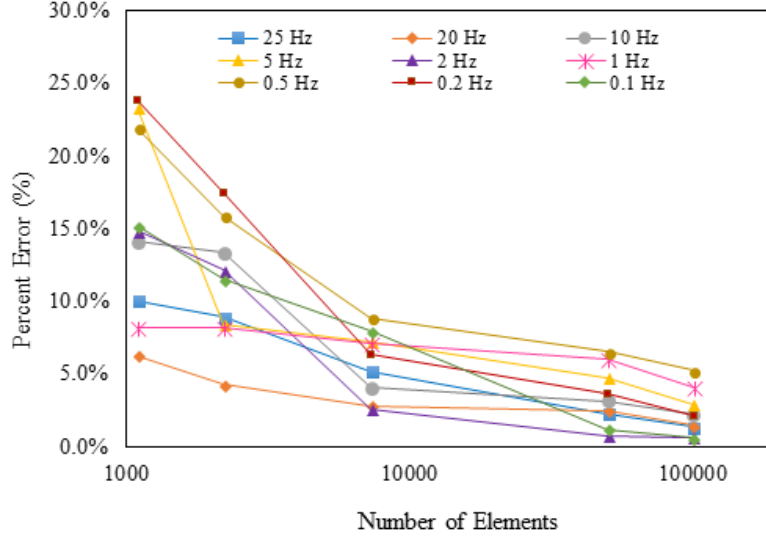
Figure 9: Convergence study results for finite element analysis

should be properly discretized or a proper order element should be selected. In order to examine the ability of selecting a proper mesh by balancing accuracy of the solution as well as computational efficiency, a mesh convergence study is performed using five different mesh sizes including 10, 7.5, 5, 2.5 and 2 mm. The result of the convergence study for the first group of asphalt mixtures is presented. Figure 9 represents a log-log scale of the relative error versus the number of elements for different loading frequencies. Based on the convergence study results, the relative error will converge to a specific value by increasing the number of elements or decreasing the mesh size.

The relative errors between simulation results and laboratory data for different loading frequencies and for different pavement sections were less than 20%, which indicates that FE modeling is a capable tool to estimate dynamic modulus and performance evaluation of asphalt concrete. Larger amount of error was observed for groups 7, 8 and 9 which means that the assumption of homogeneity for asphalt mixture is not accurate although the predicted value is not far from

the laboratory measurements.

4.4. Assessing the prediction performance: Receiver Operating Characteristics (ROC)

A receiver operating characteristics (ROC) graph is a technique for visualizing, organizing and selecting classifiers based on their performance. The ROC graphs are used widely in medical decision making as well as machine learning and data mining research [46]. The ROC curves plot the false positive rate on the x-axis and the true positive rate on the y-axis. A classifier performs well if the ROC curve climbs rapidly towards the upper left-hand corner. Random guessing on the other hand, will result in the diagonal line ($y = x$). The more the curve deviates from the $y = x$ behavior, the better the prediction is [47]. The ROC curve can be used to visualize the performance of a predictive model by plotting the error tolerance on the x-axis and the accuracy of the prediction on the y-axis. Accuracy is defined as the percentage of points that are fit within the tolerance [48]. In case of having zero tolerance, those points that the function fits exactly would be considered accurate. The obtained prediction accuracy is plotted for different error tolerances (margins) in Figure 10. The obtained curve is monotonically non-decreasing curve which climbs towards the upper left-hand corner (which is the desired situation) which shows that the predictive model performs well.

4.5. Model validation

Considering each pair of the measured and predicted dynamic modulus values, their differences are obtained from Eq. 23:

$$d_i = y_i - y_i^{'} \tag{23}$$

where y_i is the measured dynamic modulus value, $y_i^{'}$ is the predicted values, and d_i is a random error term which assumed to be normally distributed with a mean of zero and unknown variance σ^2 for i = 1, . . ., n, where n is the number of input vectors. Many types of model inadequacies and violations of the
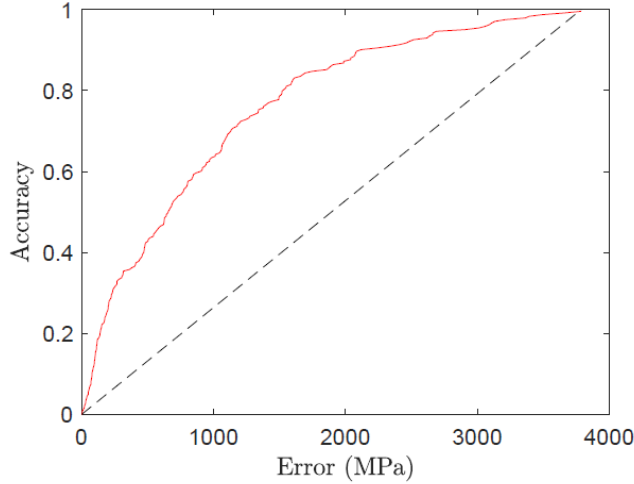
21

Figure 10: Prediction accuracy with regard to a prespecified error tolerance

underlying assumptions can be assessed. If the model is adequate, the residuals should contain no obvious pattern [49]. The plot of the difference against the predicted values is presented in Figure. 11. Since there is no obvious pattern in this plot, the assumption of equal variances seems acceptable. Figure 12 represents the linear relationship between experimental results and simulation results with the correlation coefficient of 0.98.

A histogram with a bell-shaped model over the differences (d_i) is created and presented in Figure 13. The distribution appears to be more clustered around zero than normal plot. Experimental and simulated dynamic modulus values are ploted against their mean values in Figure. 14. According to this plot although spread increases as the order of the data increase, the spread of experiment is greater than the simulation spread or the simulation method is not adding any more variation to the existing variation caused by the experiment.

5. Conclusions and recommendations

The present study used the material components' properties to estimate the dynamic modulus value by means of finite element method (FEM). Two sep-
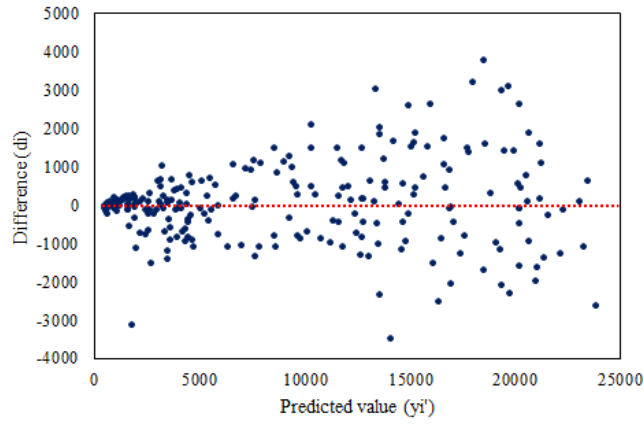
22

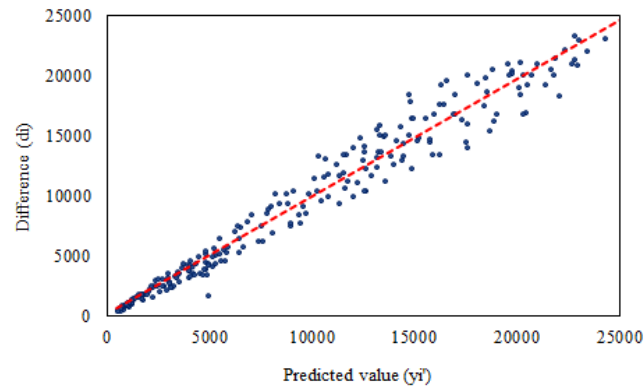Figure 11: Log of residual versus log of predicted values of dynamic modulus

Figure 12: Experimental results versus simulation results
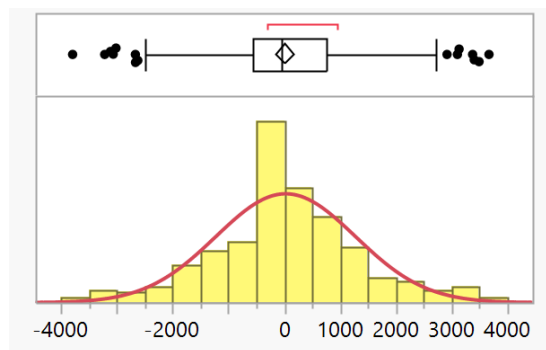

Figure 13: A histogram of the differences, d_i, with bell-shaped model overlaid
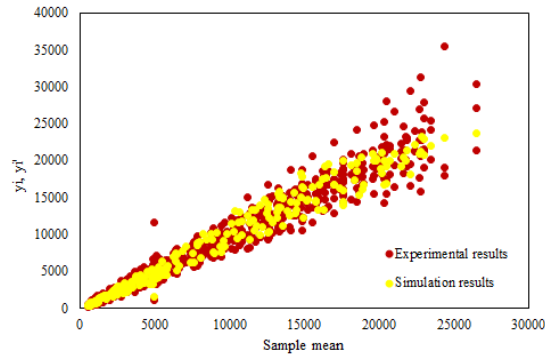
23

Figure 14: Normal distribution of the difference between two methods

arate databases were created for this research. The first one (database (a)) was created using twenty-seven field cores from nine different asphalt mixtures collected from five districts in the State of Minnesota.Database (a) contained dynamic modulus, binder shear properties, aggregate gradation and asphalt mix volumetric properties for 27 specimens. The second database (database (b)) was created using field cores taken from 20 different pavement sections in the States of Iowa, Wisconsin and Minnesota.This database is used to back-calculate the elastic modulus based on material components' properties by means of an artificial neural network. The predicted elastic modulus along with binder shear properties were used as inputs in the finite element analysis. Simulation results were compared to the experimental data in terms of the dynamic modulus master curves. Based on this comparison, FE is a capable tool in predicting dynamic modulus of asphalt mixture. In the absence of field data. ANN is able to predict/back-calculate the elastic modulus of asphalt mixture. Larger database could be more liable to be used in such predictive modeling. Although running simulation instead of performing the laboratory testing is cost effective, developing predictive models by means of machine learning techniques could be even more efficient. A larger database with more variety (location, pavement mix design, etc.) should be used in future predictive modelings.

References

[1] Kim Y, Seo Y, King M, Momen M. Dynamic modulus testing of asphalt concrete in indirect tension mode. Transportation Research Record: Journal of the Transportation Research Board 2004;(1891):163–73.

[2] Ghasemi P, Podolsky J, Christopher Williams R, Dave E. Performance evaluation of coarse-graded field mixtures using dynamic modulus results gained from testing in the indirect tension mode. In: International Conference on Transportation and Development 2016. 2016, p. 1111–21.

[3] Lin S, Ashlock JC, Williams RC. Nondestructive quality assessment of asphalt pavements based on dynamic modulus. Construction and Building Materials 2016;112:836–47.

[4] Lin S, Ashlock JC, Kim H, Nash J, Lee HD, Williams RC. Assessment of nondestructive testing technologies for quality control/quality assurance of asphalt mixtures. Tech. Rep.; 2015.

[5] Ashlock JC, Williams RC, Lee HD, Lin S, Kim H, Nash J. Assessment of nondestructive testing technologies for quality control/quality assurance of asphalt mixtures. Construction and Building Materials 2015;.

[6] Witczak M, Andrei D, Houston W. Guide for mechanistic-empirical design of new and rehabilitated pavement structures. Transportation Research Board of the National Research Council 2004;:1–91.

[7] Esfandiarpour SS, Shalaby A. Alternatives for calibration of dynamic modulus prediction models of asphalt concrete containing rap. International Journal of Pavement Research and Technology 2017;10(3):203–18.

[8] Rahman AA, Islam MR, Tarefder RA. Assessment and modification of nationally-calibrated dynamic modulus predictive model for the implementation of mechanistic-empirical design. International Journal of Pavement Research and Technology 2018;.

[9] Witczak MW. Simple performance test for superpave mix design; vol. 465. Transportation Research Board; 2002.

[10] Christensen Jr D, Pellinen T, Bonaquist R. Hirsch model for estimating the modulus of asphalt concrete. Journal of the Association of Asphalt Paving Technologists 2003;72.

[11] Al-Khateeb G, Shenoy A, Gibson N, Harman T. A new simplistic model for dynamic modulus predictions of asphalt paving mixtures. Journal of the Association of Asphalt Paving Technologists 2006;75.

[12] Junaid M, Irfan M, Ahmed S, Ali Y. Effect of binder grade on performance parameters of asphaltic concrete paving mixtures. International Journal of Pavement Research and Technology 2018;11(5):435–44.

[13] Yang JJ, Lakte PTA, Kim SH. Use of conditional inference trees for evaluating the effect of reclaimed asphalt pavement content and binder grade on the dynamic modulus of asphalt concrete mixtures. International Journal of Pavement Research and Technology 2018;.

[14] Breakah TM, Williams RC. Stochastic finite element analysis of moisture damage in hot mix asphalt. Materials and Structures 2015;48(1-2):93–106.

[15] Herzog M, Gilg A, Paffrath M, Rentrop P, Wever U. Intrusive versus non-intrusive methods for stochastic finite elements. In: From Nano to Space. Springer; 2008, p. 161–74.

[16] Duncan , M.C . Finite element analysis of pavements. Transportation Research Record: Journal of the Transportation Research Board 1968;(228):18–33.

[17] Lytton RL, Uzan J, Fernando EG, Roque R, Hiltunen D, Stoffels SM. Development and validation of performance prediction models and specifications for asphalt binders and paving mixes; vol. 357. Strategic Highway Research Program Washington, DC; 1993.

[18] Ranadive M, Tapase AB. Parameter sensitive analysis of flexible pavement. International Journal of Pavement Research and Technology 2016;9(6):466–72.

[19] Collop A, Scarpas A, Kasbergen C, de Bondt A. Development and finite element implementation of stress-dependent elastoviscoplastic constitutive model with damage for asphalt. Transportation Research Record: Journal of the Transportation Research Board 2003;(1832):96–104.

[20] Elseifi MA, Al-Qadi IL, Yoo PJ. Viscoelastic modeling and field validation of flexible pavements. Journal of engineering mechanics 2006;132(2):172–8.

[21] Akbulut H, Aslantas K. Finite element analysis of stress distribution on bituminous pavement and failure mechanism. Materials & design 2005;26(4):383–7.

[22] Breakah T. Stochastic finite element analysis of moisture damage in hot mix asphalt. Digital Repository- Iowa State University; 2009.

[23] Zhang C, Wang H, You Z, Liu Y, Yang X, Xiao J. Prediction on rutting decay curves for asphalt pavement based on the pavement-me and matter element analysis. International Journal of Pavement Research and Technology 2017;10(6):466–75.

[24] Hu X, Faruk AN, Zhang J, Souliman MI, Walubita LF. Effects of tire inclination (turning traffic) and dynamic loading on the pavement stress–strain responses using 3-d finite element modeling. International Journal of Pavement Research and Technology 2017;10(4):304–14.

[25] Ghanizadeh AR, Fakhri M. Quasi-static analysis of flexible pavements based on predicted frequencies using fast fourier transform and artificial neural network. International Journal of Pavement Research and Technology 2018;11(1):47–57.

[26] Leiva-Villacorta F, Vargas-Nordcbeck A, Timm DH. Non-destructive evaluation of sustainable pavement technologies using artificial neural

networks. International Journal of Pavement Research and Technology 2017;10(2):139–47.

[27] Flood I, Kartam N. Neural networks in civil engineering. ii: Systems and application. Journal of Computing in Civil Engineering 1994;8(2):149–62.

[28] Ghasemi P, Aslani M, Rollins DK, Williams RC, Schaefer VR. Modeling rutting susceptibility of asphalt pavement using principal component pseudo inputs in regression and neural networks. International Journal of Pavement Research and Technology 2018;.

[29] Ghanizadeh AR, Fakhri M. Quasi-static analysis of flexible pavements based on predicted frequencies using fast fourier transform and artificial neural network. International Journal of Pavement Research and Technology 2017;.

[30] Ghasemi P, Aslani M, Rollins DK, Williams RC. Principal component analysis-based predictive modeling and optimization of permanent deformation in asphalt pavement: elimination of correlated inputs and extrapolation in modeling. Structural and Multidisciplinary Optimization 2018;doi:\bibinfo{doi}{10.1007/s00158-018-2133-x}. URL https://doi.org/10.1007/s00158-018-2133-x.

[31] Li X, Williams R. A practical dynamic modulus testing protocol. Journal of Testing and Evaluation 2015;40:1–7.

[32] Sakhaeifar MS, Kim YR, Kabir P. New predictive models for the dynamic modulus of hot mix asphalt. Construction and Building Materials 2015;76:221–31.

[33] Hondros G. The evaluation of poisson's ratio and the modulus of materials of low tensile resistance by the brazilian (indirect tensile) test with particular reference to concrete. Australian J Appl Sci 1959;10(3):243–68.

[34] Schapery R, Park S. Methods of interconversion between linear viscoelastic material functions. part iian approximate analytical method. International Journal of Solids and Structures 1999;36(11):1677–99.

[35] Saltan M, TIĞDEMİR M, KARAŞAHİN M. Artificial neural network application for flexible pavement thickness modeling. Turkish Journal of Engineering and Environmental Sciences 2002;26(3):243–8.

[36] Saltan M, Sezgin H. Hybrid neural network and finite element modeling of sub-base layer material properties in flexible pavements. Materials & design 2007;28(5):1725–30.

[37] Aslani M, Asla RN, Oftadehb R, Panahic MS. A novel hybrid simplex-genetic algorithm for the optimum design of truss structures. In: Proceedings of the world congress on engineering; vol. 2. 2010,.

[38] Rahami H, Kaveh A, Aslani M, Najian Asl R. A hybrid modified genetic-nelder mead simplex algorithm for large-scale truss optimization. Iran University of Science & Technology 2011;1(1):29–46.

[39] Matheworks T. Matlab 2012b. Matheworks, Natick, MA 2012;.

[40] Moré JJ. The levenberg-marquardt algorithm: implementation and theory. In: Numerical analysis. Springer; 1978, p. 105–16.

[41] Cheng B, Titterington DM. Neural networks: A review from a statistical perspective. Statistical science 1994;:2–30.

[42] Juang CH, Chen CJ. Cpt-based liquefaction evaluation using artificial neural networks. Computer-Aided Civil and Infrastructure Engineering 1999;14(3):221–9.

[43] Abaqus V. 6.14 documentation. Dassault Systemes Simulia Corporation 2014;.

[44] Brinson HF, Brinson LC. Characteristics, applications and properties of polymers. In: Polymer Engineering Science and Viscoelasticity. Springer; 2015, p. 57–100.

[45] Williams ML, Landel RF, Ferry JD. The temperature dependence of relaxation mechanisms in amorphous polymers and other glass-forming liquids. Journal of the American Chemical society 1955;77(14):3701–7.

[46] Fawcett T. An introduction to roc analysis. Pattern recognition letters 2006;27(8):861–74.

[47] Bi J, Bennett KP. Regression error characteristic curves. In: Proceedings of the 20th international conference on machine learning (ICML-03). 2003, p. 43–50.

[48] Marti-Vargas JR, Ferri FJ, Yepes V. Prediction of the transfer length of prestressing strands with neural networks. Computers and Concrete 2013;12(2):187–209.

[49] Montgomery DC. Design and analysis of experiments. John wiley & sons; 2017.